PHYSICAL REVIEW B VOLUME 14, NUMBER 10 15 NOVEMBER 1976

Modified electron-gas study of the stability, elastic properties, and high-pressure behavior of MgO and CaO crystals

Alan J. Cohen* and Roy G. Gordon
Department of Chemistry, Harvard University, Cambridge, Massachusetts 02138
(Received 14 June 1976)

A theoretical study of the crystal structure and bonding in the simple inorganic oxide crystals magnesium oxide and calcium oxide is reported. An *a priori* method based on an electron-gas approximation is applied to an ionic description of these crystals. The quantities calculated are the equilibrium interionic separation, the elastic constants and their pressure derivatives, the transition pressures and volume changes in high-pressure-induced phase transitions, and the thermodynamic stability of the crystal structures. Comparison with available experimental data shows good agreement, without any adjustable parameters in the theory. We conclude that the ionic description of these crystals is rather accurate for energy calculations, provided that a suitably stabilized oxide ion is used in the theory.

I. INTRODUCTION

There have been many recent experimental and theoretical studies of the stability, elastic properties, and high-pressure behavior of MgO and CaO crystals. These have included high-pressure hydrostatic-compression experiments on both oxides to pressures of roughly 300 kbar,[1] ultrasonic pulse-echo experiments[2-4] to determine the elastic constants and their pressure derivatives of single-crystal MgO to 10 kbar, and to temperatures in excess of the Debye temperature ($\Theta_D = 970\,^\circ$K), similar experiments on single-crystal CaO from 80 to 298 °K and to 2 kbar,[5-7] some semiempirical calculations of the "cohesive" energies[8,9] of both oxides and of the zero-pressure elastic properties[2] of MgO, quantum-mechanical studies,[3,10,11] using modified forms of Löwdin's theory,[12] of the low- and moderately-high-pressure behavior of MgO, and a detailed semiempirical study[2] of the behavior of MgO at very high pressures up to the onset of a shear instability ($C_{44} = 0$).

None of the theoretical studies of the stability of oxide crystals that appear in the literature[8-11] is complete. The problem lies in the instability of O^{2-} ions in the gas phase. Whereas oxide ions can be stabilized by a crystalline environment they are unstable in the gas phase, and decompose spontaneously according to $O^{2-}(g) \rightarrow O^-(g) + e^-$. Hence oxide crystals do not dissociate into free[13] $O^{2-}(g)$ ions. Rather, these theories have considered the process $MO(c) \rightarrow M^{2+}(g) + O^{2-}(g, V)$, where V denotes a stabilized oxide ion (see Sec. II). The energy of this process, which is certainly not well defined experimentally or by semiempirical theories, has nevertheless been calculated by a number of investigators, and called the "cohesive" energy. A more appropriate quantity for evaluation is the energy for the process $MO(c) \rightarrow M^{2+}(g) + O^-(g) + e^-$, henceforth referred to as the binding energy. Unlike the cohesive energy, the binding energy is experimentally accessible and well defined theoretically. In this paper we discuss, in part, the construction of suitable thermodynamic cycles,[13] of which we have theoretically evaluated the steps needed to obtain binding energies for MgO and CaO. We then compare these energies with experimental binding energies.

In addition we report the results of theoretical studies of the elastic properties and phase behavior of MgO and CaO crystals over a wide range of pressures. Our high-pressure studies have been stimulated by evidence that these oxides might be important constituents of the Earth's lower mantle,[2,14] where the pressures can reach as high as 1.4 Mbar. Hence, these studies may be helpful in characterizing the physics and composition of the earth.

We recently reported the results of a modified-electron-gas (MEG) study of the cohesive energy, equilibrium structure, elastic constants, and pressure-induced phase transitions of alkali-halide crystals.[15(a)] Our calculated results showed excellent agreement with available experimental data both at low and moderate pressures. They also provided a plausible description of the higher-pressure behavior of these crystals, at pressures in excess of the experimental hydrostatic-compression ($\lesssim$300 kbar), and ultrasonic-elastic-constant-measurement ($\lesssim$10 kbar), ranges. In the present paper we have also used an MEG approximation[15(b)] to evaluate the elastic properties and high-pressure behavior of MgO and CaO, and discuss a thermodynamic cycle, evaluated in part by MEG theory, to obtain binding energies of these oxides. One of the steps in the cycle, which was not evalu-

ated by MEG theory, involved the dissociation of a stabilized oxide ion, $O^{2-}(g, V) \rightarrow O^{-}(g) + e^{-}$. The energy of this step was evaluated, in part,[16] by a numerical integration procedure.[17]

To describe the behavior of oxide ions stabilized by a crystalline environment we have used the stabilized O^{2-} wave functions of Watson[18] (+1 well solution) and Yamashita and Asano[11] (variational). These wave functions are tested within the framework of the MEG approximation,[15(b)] by using them to study lattice constants, binding energies, elastic constants and their zero-pressure derivatives, and the high-pressure behavior of MgO and CaO, and by appropriately comparing these results with the best available experimental values.

In Sec. II we discuss these wave functions in detail, describe the results of MEG studies of internuclear separations using them, and conclude with a discussion of thermodynamic cycles, the energy of the process $O^{2-}(g, V) \rightarrow O^{-}(g) + e^{-}$, and binding energies. In Sec. III the elastic properties of the oxides are discussed, and in Sec. IV a detailed treatment of the predicted high-pressure behavior of these crystals is presented. A brief summary appears as Sec. V.

II. STUDIES OF THE STABILITY OF MgO AND CaO

A. Choice of wave functions

The two basic assumptions of the original Gordon-Kim electron-gas model[19] for interactions between closed-shell systems were that the total electron density is the sum of the two separate densities, and that the non-Coulombic part of the interaction potential may be evaluated by an electron-gas treatment, using expressions for an infinite spin-paired electron gas. In a recent paper[15(a)] we used a modified version[15(b)] of this procedure (MEG model) in which the kinetic-, exchange-, and correlation-energy contributions to the short-range ion-ion interaction potentials $V_s(R)$ were appropriately corrected. The correction factors used in the present study appear in Table I.

To determine the charge densities of the cations in these oxides the Hartree-Fock (HF) wave functions of Clementi[20] were used. To model oxide ions stabilized by a crystalline environment we decided, partly on the basis of preliminary studies,[21] to use the wave functions of Watson[18] and Yamashita and Asano,[11] and to carefully test these wave functions, within the framework of the MEG method, by using them to study crystalline properties. Although other analytic HF-type O^{2-} wave functions appear in the literature[22-24] these have not been designed to describe oxide ions in crystals, but are approximations to the "free" $O^{2-}(g)$ species. Preliminary studies using some of these wave functions in an MEG model confirmed their unsuitability for crystal work.

TABLE I. Correction factors for the Gordon-Kim model.

Ion pair	Correction factors		
	Kinetic	Exchange	Correlation
$Mg^{2+}Mg^{2+}$	1.075	0.819	0.510
$Ca^{2+}Ca^{2+}$	1.060	0.962	0.580
$Mg^{2+}O^{2-}$	1.075	0.819	0.510
$Ca^{2+}O^{2-}$	1.068	0.916	0.550
$O^{2-}O^{2-}$	1.075	0.819	0.510

The Watson wave function that we used was his analytic HF solution for $O^{2-}(^1S)$ stabilized by a sphere of +1 charge with a radius of 2.66 a.u., the ionic radius.[18] The main effect of this stabilizing "shouldered-well" potential is to destroy the repulsion, due to the net charge of −1, that an electron would otherwise feel at sufficiently long distance from the nucleus and other electrons.

Yamashita and Asano[11] incorporated stabilization in another manner. They used the $(1s)^2(2s)^2$ core of Watson's +1 well solution, but described the $(2p)^6$ behavior of oxide ions in crystals by variational (double-zeta-type) wave functions. One function contained parameters to be determined by placing the O^{2-} ion in the field of six nearest neighbor Mg^{2+} ions and then minimizing the crystal energy within the framework of the Löwdin[12] approximation. We decided to test this Yamashita and Asano function, with values[11] of $p = 2.9$, $q = 1.25$, and $B = 0.17$, in our MEG studies.

It should be mentioned that Yamashita and Asano only used their wave function to determine "cohesive energies" and internuclear separations, and did not investigate the elastic properties of oxide crystals. Hence, our present study represents another test of this wave function, within the framework of the MEG method.

In Fig. 1 we present a comparison of the radial $2p$ functions $P(r)$ (see Yamashita and Asano[11] for notation), of Watson and of Yamashita and Asano, used in our electron-gas studies, along with that of Rossky's[16] numerical solution described in Sec. II C. The Yamashita and Asano function is seen to peak very sharply at roughly 1 a.u. from the nucleus, and then to cut off quite rapidly. The Watson function is more diffuse, has a smaller peak near the nucleus, and has a long tail that extends past 10 a.u. The different behavior of these wave functions is, of course, a consequence of the different stabilization procedures from which they arose. The six counterions used by Yamashita and Asano, for example, would be

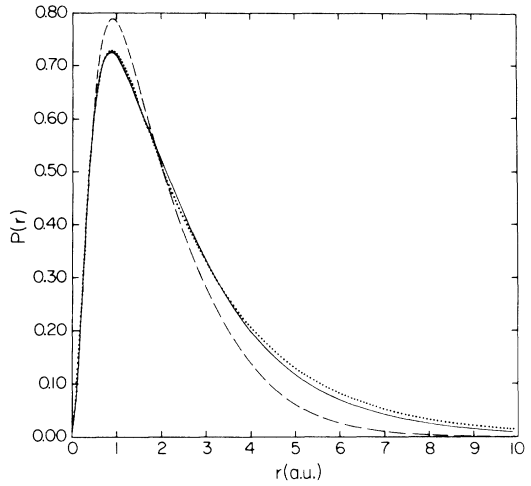

FIG. 1. Radial $2p$ wave functions for stabilized O^{2-} ions. (See Ref. 11 for notation.) Dashed line Yamashita and Asano (Ref. 11); solid line, Watson (Ref. 18); dotted line, Rossky's numerical solution (Ref. 16).

expected to be much more effective in cutting off the O^{2-} charge distribution at large distances, than a sphere of +1 charge would. In fact, our MEG studies of crystalline properties using the Yamashita and Asano wave function indicate that it gives rise to an electron distribution which is too contracted.

We have found the MEG short-range cation-anion potentials $V_s(R)_{M^{2+}O^{2-}}$ using Watson's solution, where R is the interionic separation, to be much larger than those calculated from Yamashita and Asano's solution, over a wide range of internuclear separations, and in particular for $R > 4$ a.u. in MgO. In Table II we present sample data for MgO. This behavior can be easily explained. The cations only really see the tail of the O^{2-} distributions, except at very short internuclear separations, because these cations have small effective sizes; and the O^{2-}-tail–Mg^{2+} short-range interaction, in an electron-gas model, is positive over a wide range of separations since the interaction electron density is usually sufficiently high for the positive kinetic-energy term to dominate the negative exchange- and correlation-energy terms.[15(b),19] Since the Watson function has a more extended tail than the Yamashita and Asano solution, the Watson function is expected to give rise to a more positive interaction energy. As a consequence, for electron-gas crystal studies which incorporate short-range forces for only the first-nearest-neighbor (cation-anion) pairs, one would expect a smaller cohesive energy (weaker binding) using Watson's solution than for Yamashita and Asano's. In Sec. II C this is shown to be the case.

TABLE II. Modified-electron-gas short-range potentials for Mg^{2+}-O^{2-}.

R (a.u.)	$V_s(R)$ (a.u.) Yamashita and Asano [a]	$V_s(R)$ (a.u.) Watson [b]
2.6	0.4814	0.6108
2.8	0.3230	0.4337
3.0	0.2168	0.3096
3.2	0.1454	0.2221
3.4	0.9753×10^{-1}	0.1600
3.6	0.6531×10^{-1}	0.1159
3.8	0.4365×10^{-1}	0.8423×10^{-1}
4.0	0.2910×10^{-1}	0.6148×10^{-1}
4.2	0.1933×10^{-1}	0.4505×10^{-1}
4.4	0.1279×10^{-1}	0.3314×10^{-1}
4.6	0.8429×10^{-2}	0.2447×10^{-1}
4.8	0.5524×10^{-2}	0.1814×10^{-1}
5.0	0.3600×10^{-2}	0.1350×10^{-1}
5.2	0.2331×10^{-2}	0.1008×10^{-1}
5.4	0.1499×10^{-2}	0.7549×10^{-2}
5.6	0.9565×10^{-3}	0.5674×10^{-2}
5.8	0.6052×10^{-3}	0.4278×10^{-2}
6.0	0.3793×10^{-3}	0.3235×10^{-2}
6.2	0.2352×10^{-3}	0.2453×10^{-2}
6.4	0.1440×10^{-3}	0.1864×10^{-2}
6.6	0.8698×10^{-4}	0.1420×10^{-2}
6.8	0.5164×10^{-4}	0.1084×10^{-2}
7.0	0.3001×10^{-4}	0.8288×10^{-3}
7.2	0.1695×10^{-4}	0.6347×10^{-3}
7.4	0.9177×10^{-5}	0.4867×10^{-3}
7.6	0.4635×10^{-5}	0.3736×10^{-3}
7.8	0.2072×10^{-5}	0.2870×10^{-3}
8.0	0.6798×10^{-6}	0.2206×10^{-3}

[a] Yamashita and Asano's $O^{2-}(g,V)$ function was used. See Ref. 11.

[b] Watson's $O^{2-}(g,V)$ function was used. See Ref. 18.

For O^{2-}-O^{2-} interactions (second nearest neighbors in the crystal) the MEG short-range potentials are given in Table III. Here the Yamashita and Asano solution is the more positive. For a wide range of separations corresponding to the positive energy region of these potentials, this must be due to the oxide ions interacting through the inner parts of the wave functions and not through the tails. Since the Yamashita and Asano solution has a very sharply peaked $2p$ function near the nucleus, while Watson's $2p$ solution is more diffuse, positive-energy (high density) inner-region–inner-region interactions would explain the observed results. At larger distance the tail-tail interaction, which might be expected to be negative in an MEG approximation owing to the low density, would be more negative for the Watson function, since the Yamashita and Asano function has a much smaller tail and hence the net interaction is less stabilizing. Thus, over a very wide range of internuclear separations the Yamashita and Asano

solution is the more positive of the two. Consequently, upon incorporating second-nearest-neighbor short-range forces in oxide crystals one would expect a larger decrease in cohesive energy, relative to a first-nearest-neighbor model, using the Yamashita and Asano solution than the Watson one, and the results of Sec. II C support this as well.

B. Electron-gas energy expressions

In our previous study[15] we examined the pressure-induced first-order phase transformation from the $B1$ (rocksalt) lattice to the $B2$ (cesium chloride) lattice that alkali-halide crystals undergo. It is possible that under the very high pressures (~1 Mbar) that exist in the Earth's mantle that MgO and CaO might also undergo similar transitions. In order to investigate this possibility we considered energy (and later, in Sec. IV, free energy) expressions to describe both the $B1$ and $B2$ phases. Using the MEG short-range pair potentials, the energies of these phases per $M^{2+}O^{2-}$ pair, relative to the stationary separated species $M^{2+}(g)$ and $O^{2-}(g, V)$ are, in a.u.,

$$E_{B1}(R) = -(1.747\,558/R)q^2 + 6V_s(R)_{M^{2+}O^{2-}} + 6V_s(\sqrt{2}R)_{M^{2+}M^{2+}} + 6V_s(\sqrt{2}R)_{O^{2-}O^{2-}} + 8V_s(\sqrt{3}R)_{M^{2+}O^{2-}} + 3V_s(2R)_{M^{2+}M^{2+}} + 3V_s(2R)_{O^{2-}O^{2-}} + \cdots , \quad (1)$$

$$E_{B2}(R) = -(1.762\,68/R)q^2 + 8V_s(R)_{M^{2+}O^{2-}} + 3V_s(\tfrac{2}{3}\sqrt{3}R)_{M^{2+}M^{2+}} + 3V_s(\tfrac{2}{3}\sqrt{3}R)_{O^{2-}O^{2-}} + 6V_s(\tfrac{2}{3}\sqrt{6}R)_{M^{2+}M^{2+}} + 6V_s(\tfrac{2}{3}\sqrt{6}R)_{O^{2-}O^{2-}} + 24V_s(\tfrac{1}{3}\sqrt{33}R)_{M^{2+}O^{2-}} + 4V_s(2R)_{M^{2+}M^{2+}} + 4V_s(2R)_{O^{2-}O^{2-}} + \cdots , \quad (2)$$

where R is the nearest-neighbor separation, q^2 (the charge product) is 4, and the first term in each expansion is the appropriate Madelung energy contribution.[15(a)] In Eqs. (1) and (2) short-range interactions up to fourth nearest neighbors (4NN) for the $B1$ phase, and 5NN for the $B2$ phase, have been explicitly shown. For oxides under no applied pressure the major contributions to the short-range portion of the cohesive energies of these lattices come from 1NN and 2NN, with 3NN being of greater importance in the $B2$ phase than in the $B1$ phase. Similar results were observed in our study of alkali halides, where we also rationalized this behavior on physical grounds.[15(a)] The higher-neighbor short-range terms in these expansions only appear to be important for the very-high-pressure behavior of the oxides, as we discuss in Sec. IV. Equations (1) and (2) follow from a static-lattice approximation.[15(a)]

As we discuss in Sec. II C the binding energies of the oxides can be obtained from the cohesive energies, given by Eqs. (1) and (2) for the two phases, plus the energy for the process $O^{2-}(g, V) \rightarrow O^{-}(g) + e^{-}$. Since this second step has no R dependence one may use Eqs. (1) and (2) directly to determine the equilibrium internuclear separations of the two phases at 0 °K. The results are summarized in Table IV, where the effect of various short-range potentials is explicitly shown. The trends can be explained in terms of the discussion of Sec. II A. It is doubtful that MEG potentials for ion pairs at separations much greater than $2R$ would be reliable, so we have not included these interactions in our studies. Nevertheless, they should be negligible.

TABLE III. Modified-electron-gas short-range potentials for O^{2-}-O^{2-}.

R (a.u.) [a]	$V_s(R)$ (a.u.) Yamashita and Asano [b]	$V_s(R)$ (a.u.) Watson [c]
4.0	0.6017×10^{-1}	0.3751×10^{-1}
4.2	0.4462×10^{-1}	0.2852×10^{-1}
4.4	0.3285×10^{-1}	0.2151×10^{-1}
4.6	0.2398×10^{-1}	0.1607×10^{-1}
4.8	0.1735×10^{-1}	0.1185×10^{-1}
5.0	0.1242×10^{-1}	0.8606×10^{-2}
5.2	0.8790×10^{-2}	0.6120×10^{-2}
5.4	0.6133×10^{-2}	0.4230×10^{-2}
5.6	0.4208×10^{-2}	0.2806×10^{-2}
5.8	0.2827×10^{-2}	0.1743×10^{-2}
6.0	0.1848×10^{-2}	0.9602×10^{-3}
6.2	0.1164×10^{-2}	0.3927×10^{-3}
6.4	0.6930×10^{-3}	-0.1066×10^{-4}
6.6	0.3755×10^{-3}	-0.2892×10^{-3}
6.8	0.1670×10^{-3}	-0.4740×10^{-3}
7.0	0.3479×10^{-4}	-0.5889×10^{-3}
7.2	-0.4476×10^{-4}	-0.6525×10^{-3}
7.4	-0.8866×10^{-4}	-0.6788×10^{-3}
7.6	-0.1091×10^{-3}	-0.6788×10^{-3}
7.8	-0.1145×10^{-3}	-0.6604×10^{-3}
8.0	-0.1108×10^{-3}	-0.6299×10^{-3}
8.2	-0.1019×10^{-3}	-0.5919×10^{-3}
8.4	-0.9059×10^{-4}	-0.5495×10^{-3}
8.6	-0.7852×10^{-4}	-0.5054×10^{-3}
8.8	-0.6673×10^{-4}	-0.4612×10^{-3}
9.0	-0.5584×10^{-4}	-0.4182×10^{-3}
9.5	-0.3405×10^{-4}	-0.3199×10^{-3}
10.0	-0.1990×10^{-4}	-0.2388×10^{-3}

[a] Anion-anion distance is given here.

[b] Yamashita and Asano's $O^{2-}(g,V)$ function was used. See Ref. 11.

[c] Watson's $O^{2-}(g,V)$ function of Ref. 18 was used.

TABLE IV. Equilibrium properties of the $B1$ and $B2$ phases of MgO and CaO at 0 °K.

Crystal	Model [a]	R_e (Å) $B1$	R_e (Å) $B2$	Binding Energy [g] (kcal/mole) $B1$	Binding Energy [g] (kcal/mole) $B2$
MgO	YA [b] 1-1	2.04	2.14	822±7	791±7
	YA 2-2	2.10	2.23	804±7	757±7
	YA 2-3		2.24		757±7
	YA 3-3	2.10		804±7	
	YA 4-5	2.10	2.24	804±7	757±7
	Wat. [c] 1-1	2.25	2.38	706±7	671±7
	Wat. 2-2	2.28	2.42	703±7	661±7
	Wat. 2-3		2.43		663±7
	Wat. 3-3	2.29		701±7	
	Wat. 4-5	2.29	2.43	702±7	663±7
	Expt. [d]	2.093 [e]	•••	725±1	•••
CaO	YA 1-1	2.29	2.39	726±7	702±7
	YA 2-2	2.31	2.45	721±7	687±7
	YA 2-3		2.45		687±7
	YA 3-3	2.31		721±7	
	YA 4-5	2.31	2.45	721±7	688±7
	Wat. 1-1	2.46	2.58	645±7	617±7
	Wat. 2-2	2.47	2.62	646±7	612±7
	Wat. 2-3		2.61		615±7
	Wat. 3-3	2.48		645±7	
	Wat. 4-5	2.47	2.61	646±7	615±7
	Expt. [d]	2.405 [f]	•••	632±1	•••

[a] Notation i-j means up to ith nearest-neighbor short-range forces were considered for $B1$ phase, up to jth for $B2$ phase.

[b] Yamashita and Asano's $O^{2-}(g,V)$ wave function; Ref. 11.

[c] Watson's $O^{2-}(g,V)$ wave function; Ref. 18.

[d] Experimental R_e value at 0 °K is for a static lattice, while 298 °K value incorporates vibrational motion. Experimental energy values are discussed in Sec. II C of text.

[e] Reference 2 (0 °K).

[f] Reference 8 (298 °K).

[g] This is the energy for the process $MO(c;0\,°K) \rightarrow M^{2+}(g) + O^{-}(g) + e^{-}$. The uncertainties in the energies are discussed in Sec. II C of text.

One measure of the reliability of the 4NN MEG Watson, and Yamashita and Asano descriptions of the actual binding in the oxide crystals may be obtained by comparing the calculated equilibrium separation values R_e with experimental static-lattice 0 °K values.[2] For MgO Sammis has extrapolated high-temperature lattice data from beyond the Debye temperature ($\Theta_D = 970$ °K) to obtain a static-lattice 0 °K R_e of 2.093 Å. The Watson, and Yamashita and Asano results differ by 9.2% and 0.5%, respectively, from this value. For CaO experiments have not been performed at temperatures above $\Theta_D = 650$ °K, so that there is no available static-lattice 0 °K R_e value; however, the 298 °K value[8,9] of 2.405 Å may be used as a rough estimate, and is certainly an upper bound. The Watson, and Yamashita and Asano MEG results differ by 2.9% and −3.8% from this value. These differences are partially due to the "ionic" nature of the MEG description of the binding in these oxides. The method assumes that no distortion or rearrangement of the separate electron densities[19] occurs in the oxides, and hence covalent contributions to the binding are unaccounted for. Kittel,[25] on the other hand, shows that while the binding in MgO and CaO is predominantly ionic, there is a small covalent character.

On the basis of these internuclear-separation results alone one cannot really claim that one oxide-ion wave function is superior to the other, for it appears that good agreement with reliable literature values is obtained using either one in an MEG approximation. One must also keep in mind that even for extremely ionic crystals, such as RbF, the MEG method may show a deviation of[15(a)] about 2% from experiment for this quantity. It appears, however, that the binding energies, elastic properties, and high-pressure behavior of MgO and CaO are much better described by the Watson than by the Yamashita and Asano wave function, as we discuss in detail below, and in Secs. III and IV.

C. Thermodynamic cycle for oxides

In Fig. 2 we present a thermodynamic cycle to assess the stability of the oxides. The energy for step 1 in this cycle is the "cohesive" energy which we have evaluated, using Eq. (1) of the Sec. II B for both Watson's and Yamashita and Asano's stabilized oxide-ion wave functions. Step 2 is the dissociation process $O^{2-}(g, V; {}^1S) \rightarrow O^{-}(g; {}^2P) + e^{-}$. To compare with experiment one needs to calculate the energy sum for steps 1 and 2, and compare with the sum of the remaining steps evaluated using the most reliable[2,8,9] experimental values.

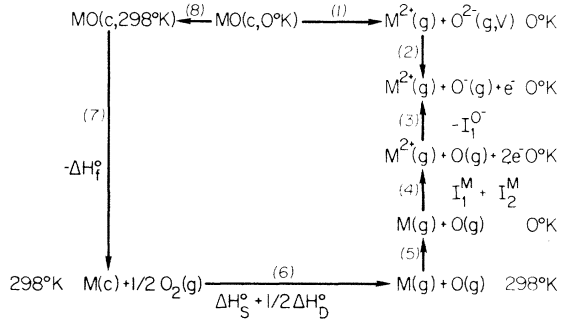

FIG. 2. Thermodynamic cycle for the oxides. The notation is discussed in detail in Sec. II C of the text. Values for steps 3–8 are given in Table V.

In Fig. 2, I_i^j is the ith ionization potential of species j, and ΔH_S^0, ΔH_D^0, and ΔH_f^0 are sublimation, dissociation, and formation enthalpies, respectively. While we have incorporated available thermal corrections at required stages in the cycle, of the order of 3 kcal/mole, it is not really necessary to apply a correction for pressure effects, since this would be extremely small. Hence, all species in the cycle may safely be assumed to be at the same pressure, 1 atm.

The best available literature values[2,8,9] for steps 3–8 for MgO and CaO are listed in Table V. The counterclockwise sum of these steps is 725 ± 1 kcal/mole for MgO, and 632 ± 1 kcal/mole for CaO, using Cantor's estimate[8] for the uncertainty in various steps to obtain an overall uncertainty.

Using Watson's oxide-ion wave function in step 1, the 4NN MEG cohesive energies for MgO and CaO were 871 and 815 kcal/mole, respectively. With Yamashita and Asano's wave function the 4NN MEG cohesive energies were 973 kcal/mole for MgO and 890 kcal/mole for CaO. There have been other *a priori* cohesive-energy calculations using these two wave functions, but within the framework of Löwdin's method.[12] When Yamashita and Asano used their wave function and considered only 1NN short-range forces, they obtained a cohesive energy of 951 kcal/mole for MgO.[11] When Calais *et al.*[10] used the Watson wave function in a 1NN Löwdin model they calculated an energy of 923 kcal/mole for MgO. These Löwdin-model results, for a particular choice of oxide-ion wave function, show good agreement with the corresponding 4NN MEG cohesive energies. It is very difficult, however, to adequately introduce second- and higher-neighbor short-range interactions in the Löwdin method; for example, when Calais *et al.*[10] included 2NN oxide-ion interactions they obtained a cohesive energy of 747 kcal/mole for MgO. They concluded that this unreasonable result was largely due to the unreasonably large oxide-ion repulsion that this theory predicted. None of these cohesive-energy values can be directly compared to any experimental quantity. Therefore, before we can test the accuracy of these theories, we must include the energy in step 2.

TABLE V. Experimental thermochemical data.

Step [a]	MgO (kcal/mole)	CaO (kcal/mole)
3	−33.8 [b]	−33.8 [b]
4	523.0 [b]	414.7 [b]
5	−2.96 [b,c]	−2.96 [b,c]
6	94.84 [b]	102.41 [b]
7	143.8 [b]	151.8 [b]
8	0.20 [d,e]	0.06 [d]
Total [f]	725 ± 1	632 ± 1

[a] These steps are shown in Fig. 2 and described in Sec. II C. The values are for the directions shown in Fig. 2.
[b] Reference 8.
[c] Ideal-gas behavior assumed.
[d] Reference 9.
[e] Reference 2.
[f] Uncertainty estimated from discussion in Ref. 8.

In any theoretical estimate of the energy of step 2 that uses a Hartree-Fock (HF) procedure the actual energy is the sum of the HF energy difference between $O^-(g;{}^2P)$ and $O^{2-}(g,V;{}^1S)$, a correlation energy difference,[23] and a relativistic energy difference.[23] The latter two terms are corrections to the accurate HF result. To describe $O^-(g;{}^2P)$ in step 2 we used the accurate Clementi HF result,[20] $E_{HF} = -74.789\,51$ a.u. (1 a.u. $\approx$ 627.5 kcal/mole). Clementi also used an extrapolation procedure[23] on atomic data and determined $E_{corr} = -0.323 \pm 0.005$ a.u., for the correlation energy. In his study of the "free" ion $O^{2-}(g;{}^1S)$ he found[23] $E_{HF} = -74.484\,42$ a.u., and $E_{corr} = -0.406 \pm 0.006$ a.u. The relativistic energy difference between his two species, O^- and O^{2-}, was negligible at -3×10^{-4} a.u., and it should be negligible for our step 2 as well. Hence, it will not be considered further in this discussion.

For our step 2 a good estimate of the correlation energy difference would be the Clementi difference between $O^-(g;{}^2P)$ and $O^{2-}(g;{}^1S)$ of 0.083 ± 0.011 a.u., for despite the fact that our dinegative ion is a stabilized ion and not a free gaseous ion, correlation energy is basically dependent upon the number (of pairs) of electrons. For example, for $F^-(g;{}^1S)$, which is isoelectronic with $O^{2-}(g;{}^1S)$, its correlation energy of[23] -0.398 ± 0.003 a.u. is extremely close to the $O^{2-}(g;{}^1S)$ value.

To evaluate the HF energy for $O^{2-}(g,V;{}^1S)$, if one wishes to obtain the HF difference in step 2, one needs a result of the same quality[16] as that of Clementi's reliable $O^-(g;{}^2P)$ calculation. Neither the Watson function ($E_{HF} = -74.383\,02$ a.u.)[26] nor that of Yamashita and Asano ($E_{HF} = -74.229\,18$ a.u.)[26] are of suitable quality (sufficiently large basis) for this step. This point was briefly discussed by Watson,[18] in the sense that he explained that by adding extra basis functions to his +1 well solution a lower $O^{2-}(g,V;{}^1S)$ HF energy could be obtained. What is desired is the HF limit value. The most reliable value to use for the HF $O^{2-}(g,V;{}^1S)$ energy appears to be the recently calculated result of Rossky,[16] and the $2p$ part of this numerical result is shown in Fig. 1. Using a numerical integration procedure,[17] with a stabilizing well of +1 charge at 2.66 a.u., he found E_{HF}

= −74.437 30 a.u. (less well energy). This result is believed to be the HF limit value.[16] It gives a HF difference of −0.352 21 a.u. for step 2, and thus a total energy of −0.269 ± 0.011 a.u. (−169 ± 7 kcal/mole) for the process.

For MgO, the theoretical sum of steps 1 and 2, using the 4NN Yamashita and Asano, and Watson MEG values for step 1, are 804 ± 7 and 702 ± 7 kcal/mole, respectively. A more complete set of data is shown in Table IV. The Watson result compares somewhat more favorably with the experimental total of 725 ± 1 kcal/mole. For CaO the Yamashita and Asano, and Watson results are 721 ± 7 and 646 ± 7 kcal/mole, with the Watson one again showing better agreement with experiment at 632 ± 1 kcal/mole. Further evidence of the reliability of the Watson MEG description of these oxides is furnished in Sec. III.

III. ELASTIC PROPERTIES OF MgO AND CaO

By studying the elastic constants C_{11}, C_{12}, and C_{44} of MgO and CaO in the $B1$ phase, and the pressure derivatives of these constants at zero pressure and 0 °K, $(\partial C_{ij}/\partial P)_0$, one gains insight into the nature of the interionic forces in these crystals. The pertinent elastic constants and derivatives are those for a static lattice at 0 °K. The importance of many-body forces[12,15(a)] can be estimated by examining deviations of the static-lattice 0 °K values of C_{12} and C_{44} from the Cauchy relation $C_{12} = C_{44}$.

The above relation holds for a cubic crystal, with ions at centers of inversion symmetry, in the absence of zero-point or thermal motion or applied pressure or other initial stresses, when the forces are of a central pairwise-additive type. For a cubic crystal, satisfying all the above criteria, but initially under hydrostatic pressure P, the appropriate relation becomes $C_{12} - C_{44} = 2P$. Here C_{ij} denotes an effective elastic constant[27] measured in a wave-propagation experiment using ultrasonic techniques on prestressed crystals. Departures from the above relations and from the static derivative relation $(\partial C_{12}/\partial P)_0 - (\partial C_{44}/\partial P)_0 = 2$ may be attributed to the presence of many-body forces in the crystals.[12]

A study of the elastic constants, and the bulk modulus B, defined by

$$B = \tfrac{1}{3}(C_{11} + 2C_{12}) \tag{3}$$

for the $B1$ phase, as a function of pressure, is also instructive. For example, the pressure at which a shear instability, $C_{44} = 0$, occurs can be taken to represent an upper bound on the transition pressure of these crystals from the $B1$ phase to a more densely packed phase, presumably $B2$, which we discuss in greater detail in Sec. IV.

To calculate the elastic constants for a static lattice at 0 °K it is useful to separate them into point-Coulombic and short-range contributions. Thus

$$C_{11} = C_{11}^{\text{Coul}} + C_{11}^{\text{sr}}\,, \tag{4}$$

and similarly for C_{12} and C_{44}. Closed-form expressions for these constants have been given as Eqs. (9)–(16) of our previous paper.[15(a)]

Using these expressions, and the rapidly convergent summation techniques described in our previous work,[15(a)] the point-Coulombic contributions to the elastic constants of MgO and CaO now become

$$C_{11}^{\text{Coul}} = (-2.556\,04/2R^4)q^2\,, \tag{5}$$

$$C_{12}^{\text{Coul}} = (0.112\,98/2R^4)q^2\,, \tag{6}$$

$$C_{44}^{\text{Coul}} = (1.278\,02/2R^4)q^2\,, \tag{7}$$

where q^2, the charge product, is 4.

For the oxides the short-range contributions to the elastic constants come largely from 1NN, 2NN, and 3NN, with a very small 4NN contribution which is important only under extremely-high-pressure conditions. Thus the short-range contributions, up to 4NN, have been obtained by explicitly expanding Eqs. (9)–(11) of our previous work,[15(a)] and using the MEG $V_s(R)$ potentials. Using an obvious contracted notation[15(a)] for $V_s(R)_{M^{2+}O^{2-}}$, $V_s(\sqrt{2}R)_{O^{2-}O^{2-}}$, and other pairs, we have

$$C_{11}^{\text{sr}} = \frac{1}{R}\left(\frac{d^2V_{+-}}{dr^2}\right)_R + \frac{1}{R}\left(\frac{d^2(V_{++}+V_{--})}{dr^2}\right)_{\sqrt{2}R} + \frac{1}{\sqrt{2}R^2}\left(\frac{d(V_{++}+V_{--})}{dr}\right)_{\sqrt{2}R}$$
$$+ \frac{4}{3R}\left(\frac{d^2V_{+-}}{dr^2}\right)_{\sqrt{3}R} + \frac{8}{3\sqrt{3}R^2}\left(\frac{dV_{+-}}{dr}\right)_{\sqrt{3}R} + \frac{2}{R}\left(\frac{d^2(V_{++}+V_{--})}{dr^2}\right)_{2R}\,, \tag{8}$$

$$C_{12}^{\text{sr}} = -\frac{1}{R^2}\left(\frac{dV_{+-}}{dr}\right)_R + \frac{1}{2R}\left(\frac{d^2(V_{++}+V_{--})}{dr^2}\right)_{\sqrt{2}R} - \frac{5}{2\sqrt{2}R^2}\left(\frac{d(V_{++}+V_{--})}{dr}\right)_{\sqrt{2}R}$$
$$+ \frac{4}{3R}\left(\frac{d^2V_{+-}}{dr^2}\right)_{\sqrt{3}R} - \frac{16}{3\sqrt{3}R^2}\left(\frac{dV_{+-}}{dr}\right)_{\sqrt{3}R} - \frac{1}{R^2}\left(\frac{d(V_{++}+V_{--})}{dr}\right)_{2R}\,, \tag{9}$$

$$C_{44}^{\text{sr}} = \frac{1}{R^2}\left(\frac{dV_{+-}}{dr}\right)_R + \frac{1}{2R}\left(\frac{d^2(V_{++}+V_{--})}{dr^2}\right)_{\sqrt{2}R} + \frac{3}{2\sqrt{2}R^2}\left(\frac{d(V_{++}+V_{--})}{dr}\right)_{\sqrt{2}R} + \frac{4}{3R}\left(\frac{d^2V_{+-}}{dr^2}\right)_{\sqrt{3}R} + \frac{8}{3\sqrt{3}R^2}\left(\frac{dV_{+-}}{dr}\right)_{\sqrt{3}R} + \frac{1}{R^2}\left(\frac{d(V_{++}+V_{--})}{dr}\right)_{2R}, \tag{10}$$

where r is the appropriate distance variable for each pair. The MEG results for the elastic constants and B at zero pressure, and their pressure derivatives, calculated using Watson's[18] and Yamashita and Asano's wave functions,[11] appear in Table VI. The MEG pressure derivatives were evaluated by a finite-difference approximation from MEG elastic constants in the 0–15-kbar range.

From Table VI, it is evident that 1NN and 2NN short-range forces greatly contribute to the elastic properties of the $B1$ phase of the oxides at zero pressure, that 3NN make a small short-range contribution, and 4NN make a negligibly small contribution, as do higher neighbors. The larger relative 3NN contribution using Watson's function than Yamashita and Asano's is related to the more extended nature of the Watson $2p$ wave function.

The experimental static-lattice 0 °K values for MgO in the table were obtained by Sammis,[2] who extrapolated the high-temperature elastic data of Spetzler[28] from beyond the Debye temperature ($\Theta_D = 970$ °K) to 0 °K. The experimental data for CaO are *not* for a static lattice, but rather are the single-crystal data of Bartels *et al.*[6,7] near room temperature. The rather large experimental uncertainties in the CaO data are related to the difficulty of growing sufficiently large single crystals to perform accurate ultrasonic pulse-echo measurements of their elastic properties.

TABLE VI. Static elastic properties of the $B1$ phase at 0 °K. (For those values *not* for a static lattice at 0 °K, the temperatures are shown in parentheses.)

Crystal	Model [a]	(kbar) C_{11}	C_{12}	C_{44}	B	$\left(\frac{\partial C_{11}}{\partial P}\right)_0$	$\left(\frac{\partial C_{12}}{\partial P}\right)_0$	$\left(\frac{\partial C_{44}}{\partial P}\right)_0$	$\left(\frac{\partial B}{\partial P}\right)_0$
MgO	YA 1	5085	1842	1842	2923	8.59	1.84	−0.16	4.09
	YA 2	4084	2185	2185	2818	7.77	2.40	0.39	4.19
	YA 3	4071	2207	2207	2828	7.73	2.43	0.43	4.20
	YA 4	4097	2208	2208	2837	7.77	2.43	0.43	4.21
	Sammis [b]	2680	1190	1190		7.8	2.0	0.003	3.9
	La and Barsch [c]						1.39	0.48	3.40
	Calais [d]	2400	590	620	1190				
	Wat. 1	2551	1259	1259	1689	7.75	1.98	−0.016	3.90
	Wat. 2	2231	1370	1370	1690	7.36	2.28	0.28	3.97
	Wat. 3	2232	1419	1419	1690	7.20	2.41	0.41	4.01
	Wat. 4	2257	1424	1424	1702	7.24	2.41	0.41	4.02
	Expt. [e]	3100	960	1600	1688	8.7	1.5	1.0	3.8
CaO	YA 1	3685	1171	1171	2009	8.60	1.78	−0.22	4.05
	YA 2	3473	1323	1323	2040	8.41	2.14	0.14	4.23
	YA 3	3481	1332	1332	2048	8.41	2.17	0.17	4.25
	YA 4	3486	1333	1333	2050	8.42	2.17	0.17	4.25
	Wat. 1	2137	882	882	1300	8.16	1.90	−0.10	3.99
	Wat. 2	2099	940	940	1326	7.96	2.08	0.081	4.04
	Wat. 3	2060	968	968	1332	7.87	2.19	0.19	4.08
	Wat. 4	2072	971	971	1338	7.89	2.19	0.19	4.09
	Expt. (298) [f]	2230 [g]	590 [g]	810	1140	10.5 [g]	3.7 [g]	0.6	6.0
				±20	±90			±0.1	±1.3

[a] YA i and Wat. i are modified electron-gas models with up to ith nearest neighbors using Yamashita and Asano's (Ref. 11), or Watson's (Ref. 18), O^{2-} wave function.

[b] Reference 2. $\mathfrak{F} = 0.7$ model, partly scaled to experiment.

[c] Reference 3. Quantum calculations except for $(\partial B/\partial P)_0$, which is a semiempirical estimate.

[d] Reference 10. Quantum calculation.

[e] Reference 2. An extrapolation of data from Ref. 28.

[f] References 6 and 7. A discussion of the large uncertainties is given in Sec. III.

[g] Uncertainties not given by authors or difficult to estimate.

The uncertainties in the C_{12} and $(\partial C_{12}/\partial P)$ data are probably very large, since C_{12} is not directly measurable in a wave-propagation experiment[27]; however, Bartels *et al.* did not estimate these uncertainties. Since there have been no high-temperature experiments on CaO (and $\Theta_D = 650$ °K),[5] one cannot obtain experimental 0 °K static-lattice values. Hence, only a very rough comparison of the MEG calculations with available experimental data may be made for this crystal, and the departure from the Cauchy relation cannot be rigorously examined since all the available data contain thermal and zero-point motion effects.

Nevertheless, on the basis of the cation-to-anion radius ratios in these oxides ($r_{Ca^{2+}}/r_{O^{2-}} > r_{Mg^{2+}}/r_{O^{2-}}$),[6] and by studying the importance of many-body forces in the isoelectronic and isostructural NaF-KF-RbF series,[15(a)] MgO is expected to exhibit a much greater departure from the Cauchy relation than CaO. Table VI shows this to be the case, if one considers the 298 °K CaO results to provide a rough indication of many-body effects in that crystal. Since our MEG calculations assumed the binding in the crystals to be of a two-body pairwise-additive type, one cannot really expect very good agreement for all of the elastic constants and their pressure derivatives with experimental data for MgO. What one would hope to calculate would be a very accurate description of the two-body force contribution to these quantities, and perhaps a good estimate of the bulk modulus of the crystal.

Prior to our present study, the most extensive two-body force-model studies of the elastic constants and their pressure derivatives of MgO were those of Sammis.[2] He used a variety of semiempirical models which incorporated 1NN short-range interactions evaluated, in part, using experimental static-lattice B and R_e values, and included 2NN anion-anion interactions by a rough Lennard-Jones 12, 6 potential. The various models differed in their evaluation of the point-Coulombic contributions to the elastic properties. Sammis multiplied Eqs. (5)–(7) by an empirical ionicity factor $\mathfrak{F}$. By varying $\mathfrak{F}$ from 0.6 to 1.0 he found that the derivative of the bulk modulus, the elastic constants, and some of their pressure derivatives showed closest agreement, on the average, with experiment for $\mathfrak{F} = 0.7$. We summarize his results in Table VI. It should be noted that if $\mathfrak{F} = 0.7$ is used to evaluate the binding energy[2] of MgO, the good agreement with experiment is now completely lost. Since we have shown that the MEG-Watson approximation gives a very good estimate for the binding energies and internuclear separations in oxide crystals, and since Table VI indicates that the model provides quite a reliable approximation for some of the elastic properties as well, it seems more consistent to study the properties of oxide crystals by this model than by a superposition of semiempirical methods with different empirical scaling factors introduced at various stages to describe different crystalline properties.

From the table it is evident that the Watson wave function provides a *much* better description of the elastic properties of oxide crystals than the Yamashita and Asano function does. Indeed, the latter function appears to be *completely inappropriate* for studying the elastic constants of these crystals and even their bulk moduli, since the calculated values show very poor agreement with experiment. On the other hand, the 4NN Watson-MEG method provides, on the average, about as reliable a description of the elastic properties as the scaled Sammis method does. In fact, the bulk modulus is extremely well predicted (0.85% error), as are the shear constant C_{44} (−11.0%) and the pressure derivative of the bulk modulus (5.8%), and these are the crucial parameters that govern the high-pressure behavior of the oxides, and are of considerable importance in geophysical studies[2,14] of the Earth's mantle. The $(\partial C_{44}/\partial P)_0$ value, also important in high-pressure work, is poor but of the same magnitude as that calculated by La and Barsch[3] using a scaled Löwdin[12] theory, which incorporated many-body effects. The C_{11} value is also about as well predicted by the MEG-Watson model as by the unscaled Löwdin model of Calais *et al.*,[10] which also included many-body effects.

The reliability of the Watson, and Yamashita and Asano descriptions of the high-pressure elastic properties of the oxides, in an MEG approximation, is discussed in Sec. IV, and a comparison with Sammis's[2] calculations using his $\mathfrak{F} = 0.7$ scaled model to describe high-pressure behavior is also presented.

IV. HIGH-PRESSURE BEHAVIOR

There has been considerable interest in developing accurate theoretical models to describe the high-pressure behavior of crystals and, in particular, oxides. This is largely due to the pressure limitations of the most reliable present experimental techniques used to monitor high-pressure compression behavior and elastic properties. Hydrostatic compression experiments on MgO and CaO have been performed, by Perez-Albuerne and Drickamer,[1] only up to pressures of 350 and 250 kbar, respectively, with the compression proceeding isothermally. Although, in principle, shock-wave methods may be used to study crystal

behavior at higher pressures, these experiments are not always reliable, and the data, which correspond neither to an adiabatic nor isothermal compression, proves difficult to correct to an adiabat or isotherm.[2] Similarly, measurements of effective elastic constants and their pressure derivatives are limited, using present ultrasonic pulse-echo techniques on single crystals,[28] to low pressures of roughly 10 kbar. The possibility of determining these elastic properties by Brillouin scattering techniques on single-crystal samples in diamond-anvil high-pressure compression cells, which is now under investigation,[29] would greatly extend the pressure range over which these properties could be monitored. There would still be, however, a need for accurate theoretical models to provide insight into higher-pressure (> 300 kbar) behavior.

In our previous study[15(a)] we tested our MEG model on alkali-halide crystals and found that it provided a very good description of the behavior of the $B1$ (rocksalt) phase of these crystals at relatively high pressures. This is in part related to the accuracy of the model in describing the forces between a pair of ions when they are at short separations from each other.[19] We expect the MEG model for oxides, using the more reliable Watson function, to provide a reasonable description of the high-pressure behavior of the oxides as well.

In Figs. 3 and 4 the MEG compression results, using Watson's and Yamashita and Asano's wave functions, are presented, together with Perez-Albuerne and Drickamer's[1] experimental data. In

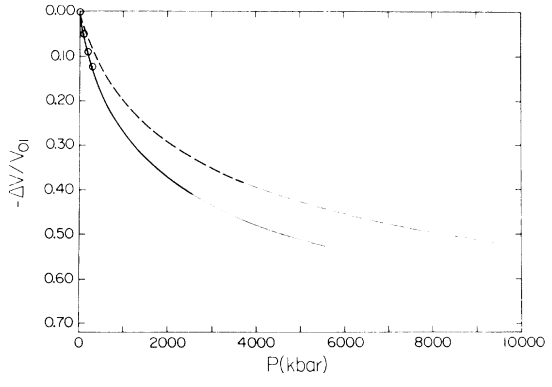

FIG. 3. Compression curve for the $B1$ phase of MgO. Dashed curve calculated, including up to 4NN, using Yamashita and Asano's O^{2-} function; solid curve calculated, including up to 4NN, using Watson's O^{2-} function. Dark lines indicate regions of stability and light lines regions of metastability. Experimental data (shown as circles) from Perez-Albuerne and Drickamer, Ref. 1.

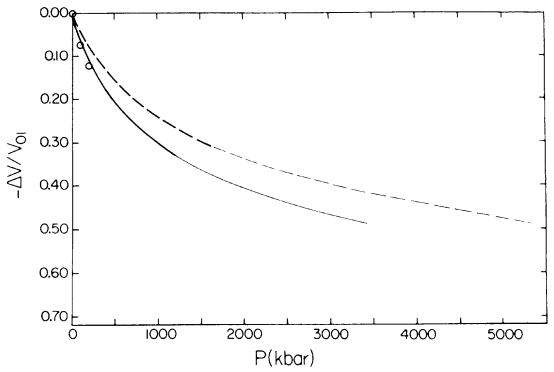

FIG. 4. Compression curve for the $B1$ phase of CaO. Experimental data from Ref. 1. Other notation as in Fig. 3.

these figures, $-\Delta V/V_{01}$, the "relative-volume" factor, is $1 - V/V_{01}$, where V_{01} is the volume of the $B1$ phase at zero pressure, and V the volume at pressure P. These relative-volume factors were determined from the equilibrium internuclear separations in the crystals at P, evaluated by minimizing the Gibbs free energy of the $B1$ phase. The Gibbs free energy at 0 °K is given by

$$G(R) = E(R) + 2R^3P\,, \tag{11}$$

where $E(R)$ is given by the full equation (1), up to 4NN short-range interactions. Compression curves calculated using only 1NN short-range interactions[30] showed some deviation from those using 2NN short-range interactions; however, there was little difference in the $B1$ curve when 3NN or 4NN were added. This is consistent with the results presented in Sec. III for the bulk modulus and its pressure derivative in these crystals. These elastic-property results largely converged after 2NN short-range interactions were added, and these are the parameters that determine the shape of the compression curves for the lower-pressure region of a few hundred kbar.

The excellent agreement with available experimental data for both oxides for the MEG-Watson model, is also partly a consequence of the quality of the predictions of B and $(\partial B/\partial P)_0$ by this model. The MEG–Yamashita-Asano compression curves change too slowly with pressure, showing poor agreement with experiment, because the bulk moduli predicted by this model are too large. The actual crystals are much less rigid than this model predicts.

As in our previous work[15(a)] we have extended the compression curves to regions of metastability. The solid lines in the figures show the stable-

phase behavior of these crystals and terminate at the transition pressure, where the $B1$ (rocksalt) lattice is in equilibrium with the $B2$ (cesium chloride) lattice. The lighter regions, which extend past the transition pressure, are domains for which the $B1$ phase is metastable.[15(a)] These lines, in turn, terminate at the shear instabilities, where the shear constant C_{44}, for the [100] direction vanishes, and the crystals become unstable to homogeneous deformation.[31,32]

We have determined both the transition pressures and shear instabilities of these crystals, and the results are summarized in Table VII, where the effect of various nearest neighbors is explicitly shown. To determine the transition pressures it was necessary to study the phase behavior of the $B2$ lattice, described by

$$G(R') = E(R') + (8/3\sqrt{3})(R')^3 P , \tag{12}$$

where R' is the $B2$ internuclear separation at P, and $E(R')$ is determined by Eq. (2). When 4NN were included in the $B1$ phase and 5NN in the $B2$ phase the transition pressures for MgO were 2560 kbar for the Watson function and 3720 kbar for the Yamashita and Asano function. For CaO the Watson result was 1210 kbar, and the other function predicted a transition at 1620 kbar. There was a problem with convergence for the MgO Watson calculation, perhaps partially due to an incomplete description of the $B2$ phase, and to the diffuse nature of the Watson $2p$ wave function; however, this is not the crucial point. The important point is that the models predict that the polymorphic phase transitions for these oxides occur at pressures either near (for CaO) or above (for MgO) the 1.4-Mbar pressure limit, which is the pressure at the core-mantle boundary in the Earth.[14] This result has geophysical significance. We believe that the Watson curves also present a reasonable description of the high-pressure $B1$-phase behavior of these oxides in the mantle, and hence may also be of interest to geophysicists.

To determine the shear instabilities and to monitor the high-pressure behavior of all the effective elastic constants, the equations developed in Sec. III were evaluated at the appropriate equilibrium separations. From the discussion in Sec. III, the MEG C_{44} results are probably much better than our C_{11} and C_{12} predictions. The results for MgO appear as Figs. 5–7, and for CaO as Figs. 8–10. In the figures for C_{44} we present both 2NN and 4NN (virtually identical to 3NN) curves to show that only at pressures above 1 Mbar do the 3NN interactions make significant contributions. For MgO we have compared our results to those of Sammis,[2] who used his $\mathcal{F} = 0.7$ model (including up to 2NN), discussed in Sec. III, to monitor high-pressure elastic properties, and to locate the shear instability.

We believe that our MgO C_{44} curve, calculated using up to 4NN with Watson's oxide wave function, provides at least as satisfactory a description of the high-pressure behavior of MgO as Sammis's $\mathcal{F} = 0.7$ curve does, and perhaps better. One reason is that our C_{44} zero-pressure value, and its pressure derivative, are more accurate than Sammis's and these parameters govern the linear, lower-pressure regions of the curve. Of greater importance is that although Sammis's model has been very well fit to experiment, the fit was at zero pressure. Expansions containing zero-pressure experimental quantities have a limited range of applicability and may fail at a sufficiently high pressure. The electron-gas model, on the other hand, usually provides a good description of forces in crystals even when the pressure is increased,[15(a)] as we have discussed. Thus it is hoped that the high-pressure MEG predictions, using Watson's wave function, might provide useful estimates of the actual high-pressure behavior of these oxide crystals.

TABLE VII. High-pressure behavior of MgO and CaO.

Crystal	Model [a]	Transition pressure (kbar) [b]	Shear instability of $B1$ phase ($C_{44}=0$) (kbar) [b]
MgO	YA 1-1	1510	3400
	YA 2-2	3180	7550
	YA 2-3	4020	
	YA 3-3	3720	9450
	YA 4-5	3720	9325
	Wat. 1-1	2040	2575
	Wat. 2-2	2940	3875
	Wat. 2-3	3060	
	Wat. 3-3	2060	5575
	Wat. 4-5	2560 [c]	5550
CaO	YA 1-1	750	2090
	YA 2-2	1620	4300
	YA 2-3	1670	
	YA 3-3	1650	5400
	YA 4-5	1620	5375
	Wat. 1-1	960	1700
	Wat. 2-2	1520	2475
	Wat. 2-3	1370	
	Wat. 3-3	1130	3425
	Wat. 4-5	1210	3425

[a] Same notation as in Table IV.

[b] These results were determined to within 1% uncertainty.

[c] Convergence problem is discussed in Sec. IV of text.

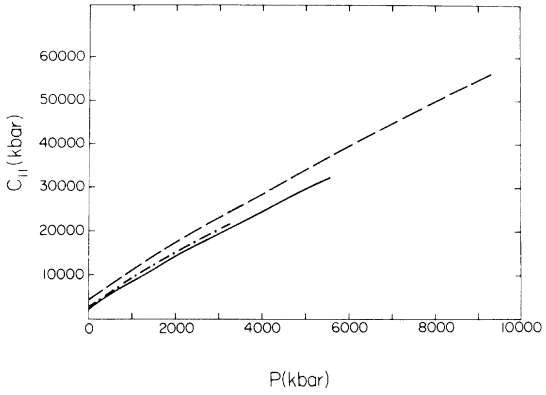

FIG. 5. Pressure variation of C_{11} in the $B1$ phase of MgO. Dashed curve calculated, including up to 4NN, using Yamashita and Asano's O^{2-} function; solid curve calculated, including up to 4NN, using Watson's O^{2-} function; dash-dot curve, Sammis's $\mathfrak{F}=0.7$ calculation, given in Ref. 2.

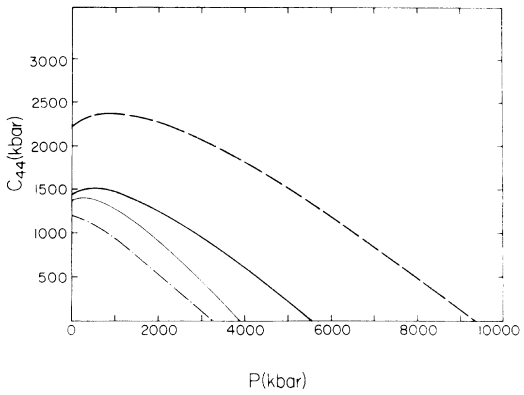

FIG. 7. Pressure variation of C_{44} in the $B1$ phase of MgO. Notation as in Fig. 5, except light solid curve was calculated using Watson's O^{2-} function, but only including up to 2NN.

V. SUMMARY

A modified-electron-gas approximation, using Watson's +1 well solution to describe oxide ions stabilized in a crystalline environment,[18] gave very good agreement with available experimental data on properties of MgO and CaO. The internuclear separation, the sum of the "cohesive" energy and the energy for the process $O^{2-}(g, V) \rightarrow O^{-}(g) + e^{-}$ (which we have called the binding energy), some of the important elastic properties, and the high-pressure behavior, of these crystals, were well predicted.

When the variational oxide-ion wave function of Yamashita and Asano[11] was used in a modified electron-gas approximation most of the good agreement with experiment was lost. This wave function gave rise to lattices that were too stable and much too rigid. This is largely a consequence of the method by which Yamashita and Asano stabilized their oxide ion, which resulted in too contracted an electron distribution.

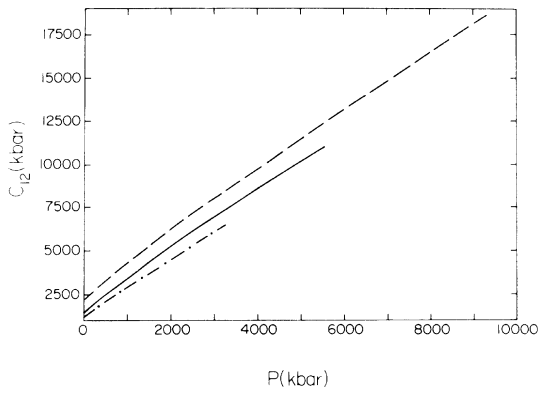

FIG. 6. Pressure variation of C_{12} in the $B1$ phase of MgO. Notation as in Fig. 5.

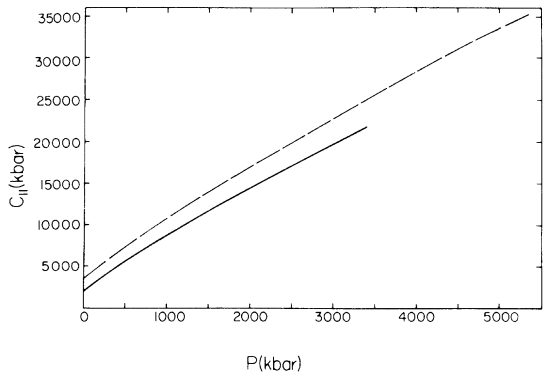

FIG. 8. Pressure variation of C_{11} in the $B1$ phase of CaO. Dashed curve calculated, including up to 4NN, using Yamashita and Asano's O^{2-} function; solid curve calculated, including up to 4NN, using Watson's O^{2-} function.

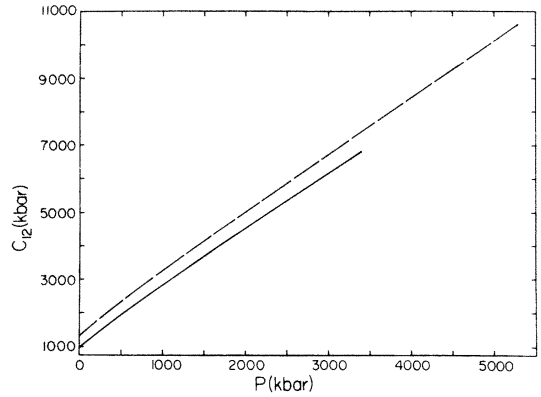

FIG. 9. Pressure variation of C_{12} in the $B1$ phase of CaO. Notation as in Fig. 8.

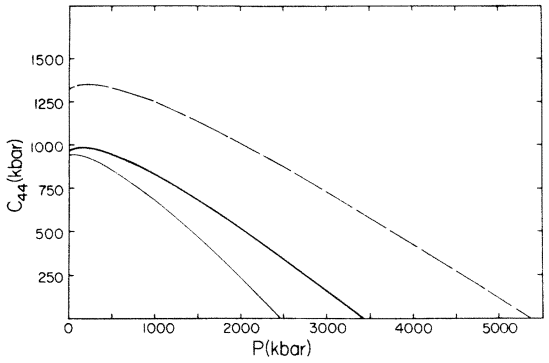

FIG. 10. Pressure variation of C_{44} in the $B1$ phase of CaO. Notation as in Fig. 8, except light solid curve was calculated using Watson's O^{2-} function, but only including up to 2NN.

ACKNOWLEDGMENTS

We would like to thank Peter Rossky for several very useful discussions, Richard M. Stevens for the use of POLYCAL, and Marvin Waldman and Michael Clugston for helpful comments. Some of the work on high-pressure oxide behavior was stimulated by discussions with Professor Richard J. O'Connell of the Geology Department at Harvard.

---

*Supported by a John Parker Fellowship.

[1]E. A. Perez-Albuerne and H. G. Drickamer, J. Chem. Phys. 43, 1381 (1965).

[2]C. G. Sammis, Ph.D. thesis (California Institute of Technology, 1971) (unpublished), and references therein.

[3]S. Y. La and G. R. Barsch, Phys. Rev. 172, 957 (1968), and references therein.

[4]H. A. Spetzler and D. L. Anderson, J. Am. Ceram. Soc. 54, 520 (1971).

[5]H. E. Hite and R. J. Kearney, J. Appl. Phys. 38, 5424 (1967).

[6]P. R. Son and R. A. Bartels, J. Phys. Chem. Solids 33, 819 (1972).

[7]R. A. Bartels and V. H. Vetter, J. Phys. Chem. Solids 33, 1991 (1972).

[8]S. Cantor, J. Chem. Phys. 59, 5189 (1973), and references therein.

[9]E. Gaffney and T. J. Ahrens, J. Chem. Phys. 51, 1088 (1969).

[10]J. L. Calais, K. Mansikka, G. Pettersson, and J. Vallin, Ark. Fys. 34, 361 (1967).

[11]J. Yamashita and S. Asano, J. Phys. Soc. Jap. 28, 1143 (1970).

[12]P. O. Löwdin, Ph.D. thesis (Uppsala, 1948) (unpublished).

[13]See the discussion in D. R. Herrick and F. H. Stillinger, J. Chem. Phys. 62, 4360 (1975), and references therein.

[14]F. D. Stacey, *Physics of the Earth* (Wiley, New York, 1969), Chaps. 1 and 4.

[15](a) A. J. Cohen and R. G. Gordon, Phys. Rev. B 12, 3228 (1975), and references therein; (b) M. Waldman and R. G. Gordon (unpublished).

[16]P. Rossky (private communication).

[17]C. Froese, Can. J. Phys. 41, 1895 (1963).

[18]R. Watson, Phys. Rev. 111, 1108 (1958).

[19]R. G. Gordon and Y. S. Kim, J. Chem. Phys. 56, 3122 (1972).

[20]E. Clementi and C. Roetti, At. Data Nucl. Data Tables 14, 177 (1974).

[21]R. G. Gordon (unpublished).

[22]S. Huzinaga and A. Hart-Davis, Phys. Rev. A 8, 1734 (1973).

[23]E. Clementi and A. D. McLean, Phys. Rev. 133, A419 (1964).

[24]R. Ahlrichs, Chem. Phys. Lett. 34, 570 (1975).

[25]C. Kittel, *Introduction to Solid State Physics*, 4th ed. (Wiley, New York, 1971), Chaps. 3 and 4.

[26]We report these values, which we obtained in part by using the POLYCAL program of Stevens [R. M. Stevens, J. Chem. Phys. 61, 2086 (1974)], because Yamashita and Asano did not publish an energy value, and Watson's result, published in Ref. 18, appears to be inaccurate. In both cases we report the HF energies for renormalized wave functions.

[27]D. C. Wallace, Phys. Rev. 162, 776 (1967).

[28]H. Spetzler, J. Geophys. Res. 75, 2073 (1970).

[29]D. J. Weidner, K. Swyler, and H. R. Carleton, Geophys. Res. Lett. 2, 189 (1975).

[30]A. J. Cohen (unpublished).

[31]M. Born, Proc. Camb. Philos. Soc. 36, 160 (1940).

[32]O. L. Anderson and R. C. Liebermann, Phys. Earth Planet. Inter. 3, 61 (1970).